

Polymer Chemistry

Accepted Manuscript



This is an *Accepted Manuscript*, which has been through the Royal Society of Chemistry peer review process and has been accepted for publication.

Accepted Manuscripts are published online shortly after acceptance, before technical editing, formatting and proof reading. Using this free service, authors can make their results available to the community, in citable form, before we publish the edited article. We will replace this *Accepted Manuscript* with the edited and formatted *Advance Article* as soon as it is available.

You can find more information about *Accepted Manuscripts* in the [Information for Authors](#).

Please note that technical editing may introduce minor changes to the text and/or graphics, which may alter content. The journal's standard [Terms & Conditions](#) and the [Ethical guidelines](#) still apply. In no event shall the Royal Society of Chemistry be held responsible for any errors or omissions in this *Accepted Manuscript* or any consequences arising from the use of any information it contains.

ARTICLE

Injectable Enzymatically-crosslinked Hydrogels Based on Poly(L-glutamic acid) Graft Copolymer

Cite this: DOI: 10.1039/x0xx00000x

Kaixuan Ren,^{a,b} Chaoliang He,^{a,*} Yilong Cheng,^a Gao Li,^{a,*} and Xuesi Chen^aReceived 00th January 2012,
Accepted 00th January 2012

DOI: 10.1039/x0xx00000x

www.rsc.org/

Enzymatically-crosslinked injectable hydrogels based on poly(L-glutamic acid) grafted with tyramine and poly(ethylene glycol) (denoted as PLG-g-TA/PEG) were developed under physiological conditions with the presence of horseradish peroxidase (HRP) and hydrogen peroxide (H₂O₂). Their gelation time, mechanical properties, swelling behaviors and porous structure were evaluated. The hydrogels were rapidly formed with the presence of low concentrations of HRP and H₂O₂. The storage modulus of the hydrogels could be well controlled and increased with increasing the concentrations of HRP and H₂O₂. The average pore-size of the hydrogels varied from 20 to 120 μm, depending on the H₂O₂ concentration. In addition, the encapsulated L929 fibroblast cells in the PLG-g-TA/PEG hydrogels exhibited high viability and proliferation. After subcutaneous injection of the PLG-g-TA/PEG solutions containing HRP and H₂O₂ into the back of rats, the hydrogels were rapidly formed *in situ*. The hydrogels were found to persist for up to 10 weeks *in vivo*, and histological analysis indicated that the hydrogels exhibited acceptable biocompatibility. These results suggested that the biocompatible, injectable enzyme-mediated PLG-g-TA/PEG hydrogels are promising for biomedical applications including tissue engineering scaffolds and drug delivery carriers.

Introduction

Hydrogels are three-dimensional (3D) hydrophilic polymer networks retaining a large amount of water. Due to their high water contents and physical properties that resemble the native extracellular matrix (ECM), hydrogels have drawn considerable attention for biomedical applications, such as tissue engineering scaffolds and drug delivery carriers.¹⁻⁵ Injectable hydrogels exhibit unique advantages, such as excellent permeability for nutrients and metabolites, good biocompatibility and minimally invasive injection procedures. The encapsulation of cells, drugs, and bioactive molecules into the hydrogels can be easily achieved. Up to now, various crosslinking approaches, including physical and chemical crosslinking, have been developed to construct hydrogels *in situ*. Physically-crosslinked hydrogels are formed based on non-covalent interactions, such as ionic interactions,^{6, 7} hydrogen bonds,⁸ hydrophobic interactions,⁹ and stereo-complexations.^{10, 11} They are usually reversible networks with relatively low mechanical properties. On the other hand, chemically-crosslinked hydrogels are covalent networks formed *via* chemical reactions, including radical polymerization,^{12, 13} Michael-type addition reaction,¹⁴⁻¹⁶ or Schiff-base reaction.¹⁷

Recently, increasing attention has been paid to enzymatically-crosslinked hydrogels for biomedical applications due to their good

biocompatibility, fast gelation process and tunable mechanical properties. Horseradish peroxidase (HRP) is the most widely used enzyme for enzymatically-crosslinked hydrogels because of its high stability and good biocompatibility.¹⁸ HRP is a hemoprotein that catalyzes the coupling of aniline or phenol derivatives via a carbon-carbon bond or a carbon-nitrogen/oxygen bond with the presence of hydrogen peroxide.¹⁸ Additionally, the physiochemical properties of hydrogels, such as gelation rate, mechanical strength and porous structure, are easy to control by modulation of the HRP activity. Considerable studies on HRP-mediated *in-situ* forming hydrogels have been focused on naturally derived materials, such as hyaluronic acid,¹⁹⁻²¹ alginate,^{22, 23} dextran,²⁴⁻²⁷ gelatin²⁸⁻³¹ and chitosan³²⁻³⁶. These hydrogels have been shown potential in biomedical applications due to their cell-interactive properties and biodegradability. Very recently, the enzymatically-crosslinked hydrogels based on synthetic polymers have attracted increasing interest due to their advantages including tunable mechanical properties and low immunogenicity. For instance, the injectable hydrogels based on tyramine-conjugated 4-arm poly(propylene oxide)-poly(ethylene oxide) (PPO-PEO) *via* enzyme-catalyzed crosslinking have been developed.³⁷⁻⁴⁰ The hydrogels displayed good cytocompatibility and degraded rapidly in 6 days *in vitro*.³⁸

Among various synthetic polymers, synthetic polypeptides have attracted extensive interest due to their excellent biocompatibility,

biodegradability, and structures mimicking natural proteins.^{41, 42} In addition, the reactive side groups in some polypeptides facilitate further functionalization. These properties lead to unique advantages of polypeptides in biomedical applications. Nevertheless, to-date, reports on injectable enzymatically-crosslinked hydrogels based on polypeptides were still limited. In the present work, a type of injectable hydrogels based on poly(L-glutamic acid) grafted with tyramine and poly(ethylene glycol) (denoted as PLG-g-TA/PEG) were prepared under physiological conditions with the presence of horseradish peroxidase (HRP) and hydrogen peroxide (H₂O₂). The PLG-g-TA/PEG copolymers were synthesized *via* an amidation reaction. The chemical structures of the copolymers were characterized by ¹H NMR and UV-Vis spectroscopy. The physicochemical properties of the hydrogels, such as gelation time, mechanical properties, swelling behaviors and porous structure, were studied in detail. The viability and proliferation of L929 fibroblast cells in the hydrogels were evaluated by the live-dead assay and cell counting kit-8 (CCK-8) method. Moreover, the biodegradability and biocompatibility of the hydrogels *in vivo* were further investigated by subcutaneous injection of the hydrogels in the back of rats.

Experimental

Materials

Poly(ethylene glycol) monomethyl ether (mPEG, $M_n=2000$) was purchased from Aldrich. The amino-terminated poly(ethylene glycol) monomethyl ether (mPEG-NH₂) was synthesized according to the literature procedure.^{43, 44} γ -benzyl-L-glutamate-N-carboxyanhydride (BLG NCA) was synthesized according to previously reported method.⁴⁵ N-ethyl-N'-(3-dimethylaminopropyl) carbodiimide hydrochloride (EDC) (GL Biochem), N-hydroxysuccinimide (NHS) (GL Biochem), tyramine hydrochloride (TA) (Aladdin), HBr solution (33 wt%) in acetic acid (J&K Scientific Ltd) and dichloroacetic acid (CHCl₂COOH) (J&K Scientific Ltd) were used as received. Horseradish peroxidase (HRP, 200 units/mg) was purchased from Aldrich and used without further purification. Tetrahydrofuran (THF) and dioxane were refluxed with sodium and distilled under nitrogen prior to use. All the other reagents and solvents were of analytical grade and used as obtained.

Characterization

¹H NMR spectra were recorded on a Bruker AV 400 NMR spectrometer. The molecular weights and polydispersity indexes (PDI) of poly(L-glutamic acid) were determined by gel permeation chromatography (GPC) using a Waters linear Ultrahydrogel column and Waters 1515 isocratic HPLC pump with a Waters 2414 refractive index detector. The eluent was 0.2 M phosphate buffer (PB) containing 0.1 M NaNO₃ at a flow rate of 1.0 mL min⁻¹ at 25 °C. Monodispersed PEG standards purchased from Waters Co. with a molecular weight ranging from 3000 to 1.0×10⁵ were used to generate the calibration curve. The content of conjugated phenol groups within the copolymer was measured by using an ultraviolet-visible (UV-Vis) spectrometer (UV-2401PC, Shimadzu, Kyoto, Japan). The PLG-g-TA/PEG copolymer was dissolved at 1 mg/mL in distilled water and the absorbance at 277 nm was measured. The content of conjugated phenol groups was calculated from a calibration curve obtained by measuring the absorbance of tyramine hydrochloride at different concentrations in distilled water. The ellipticity of polymer aqueous solution (0.5 g L⁻¹, pH = 7.4) was obtained on a JASCO J-810 spectrometer at 25 °C.

Synthesis of poly(L-glutamic acid) (PLG)

Poly(γ -benzyl-L-glutamate) (PBLG) was synthesized according to our previously reported method.⁴⁵ Typically, BLG NCA (10.3 g, 39 mmol) was dissolved in anhydrous dioxane under nitrogen atmosphere, and triethylamine (TEA, 17.6 μ L, 0.13 mmol) was then added. The reaction mixture was allowed to stir at 25 °C for three days. Then the polymer was purified by precipitation into cold diethyl ether, followed by filtration. The obtained product was further purified with diethyl ether and dried under vacuum. PBLG was obtained with the yield of 72%. Poly(L-glutamic acid) (PLG) was obtained by deprotection of PBLG. Briefly, PBLG (5 g) was dissolved in 50 mL of CHCl₂COOH, followed by addition of 15 mL of HBr solution (33 wt%) in acetic acid. The reaction mixture was stirred at 30 °C for two hours. The product was obtained by precipitation in diethyl ether, washed repeatedly with diethyl ether and dried under vacuum. After dissolving the product in DMSO, the solution was dialyzed against deionized water for 3 days (MWCO 7000 Da). PLG was collected by lyophilization with a yield of 87%.

Synthesis of poly(L-glutamic acid)-*graft*-tyramine/poly(ethylene glycol) (PLG-g-TA/PEG)

PLG-g-TA/PEG copolymer was prepared by coupling PLG with TA and mPEG-NH₂ *via* EDC/NHS activated amidation reaction. PLG (1.5 g, 11.6 mmol of COOH groups) was first dissolved in 40 mL of DMSO. The carboxyl groups of PLG were activated using EDC/NHS (COOH:EDC:NHS = 1:0.6:0.6 (molar ratio)). TA (0.5 g, 2.9 mmol) and mPEG-NH₂ (7.0 g, 3.5 mmol) were then added and the resulting solution was stirred for two days at room temperature. The product was purified by dialysis against deionized water for 3 days (MWCO 7000 Da). The final product, PLG-g-TA/PEG copolymer, was collected as a white solid by lyophilization with a yield of 83%.

Gelation time

Enzymatically-crosslinked PLG-g-TA/PEG hydrogels (300 μ L) were prepared with the presence of HRP and H₂O₂ at room temperature. The final concentration of PLG-g-TA/PEG was fixed at 6.7% (w/v) (Figure S1 in Supporting Information). To evaluate the dependence of gelation time on the HRP and H₂O₂ concentration, the polymer solution (200 μ L, 10% (w/v)) in 0.01 M PBS (pH 7.4) was mixed with different concentrations of HRP solution (50 μ L) and H₂O₂ solution (50 μ L) in 5 mL vials, and then the mixture was gently shaken. The gelation time of the PLG-g-TA/PEG hydrogels was determined using the vial tilting method. The sample was considered to be a gel state if no flow was observed within 30 s after inverting the vial.

Rheological experiments

Rheological experiments of the hydrogels were performed on a US 302 Rheometer (Anton Paar) using a parallel plate (plate diameter = 25 mm, gap = 0.5 mm) in oscillatory mode at 37 °C. For the measurements, 200 μ L of the PLG-g-TA/PEG solution (10% (w/v)) was mixed with different concentrations of HRP solution (50 μ L) and H₂O₂ solution (50 μ L), and then placed on the plate of the rheometer immediately. The storage modulus (G') and loss modulus (G'') were recorded as a function of time at a frequency of 1 Hz and a strain of 1%. The sample was sealed by a thin layer of silicon oil to prevent the evaporation of water.

Morphology of the hydrogels

To measure the morphology of hydrogels, the samples were frozen rapidly by plunging them into liquid nitrogen and then freeze-dried for two days. The specimens were cross-sectioned and sputter coated

with gold. The morphology of the specimens was observed by scanning electron microscope (Micrion FEI PHILIPS).

Swelling ratio

Hydrogels were prepared in vials according to the procedure above. The freeze-dried hydrogels were accurately weighed (W_0) and then incubated in 10 mL of PBS solution at 37 °C. At predetermined time intervals, the buffer solutions were removed completely and the left samples were weighed (W_t) to calculate the swelling ratio (SR), which is defined as $(W_t - W_0)/W_0$. The experiments were performed in triplicate.

In vitro cytocompatibility

The cell viability and proliferation of the hydrogels was evaluated by 3D culture of L929 mouse fibroblasts inside the hydrogels. Cells were cultured in Dulbecco's modified Eagle's medium (DMEM) containing 10% fetal bovine serum, supplemented with 50 U mL⁻¹ penicillin and 50 U mL⁻¹ streptomycin and incubated at 37 °C and in 5% CO₂ atmosphere. All the sample solutions were sterilized by filtrating via 0.2 μm syringe filters. First, PLG-g-TA/PEG solution (10% (w/v), 200 μL) was mixed with harvested cells (1×10^5 cells) and put into the well of a 24-well plate, and then 50 μL of HRP solution and 50 μL of H₂O₂ solution were added into the well. 1 mL of DMEM was added after the hydrogel was formed. The viability of encapsulated L929 cells at 24h was determined by using a live-dead cell staining kit. In brief, 500 μL of PBS solution containing 2 μM calcein AM and 4 μM propidium iodide (PI) was added and the sample was further incubated at 37 °C for 30 min. The sample was observed by fluorescent microscope after removing the staining solution. Viable cells were stained green with calcein AM, and dead cells were stained red with PI. In addition, the proliferation of L929 cells in the hydrogels was assessed by cell counting kit-8 (CCK-8) method (n=3). At predetermined period, CCK-8 solution (1.0 mL, 10% v/v in medium) was added into each well of the plate. After 4h incubation, the absorbance value at 450 nm was measured with an ELISA reader (Tecan Infinite M200). The absorbance at 600 nm was used for baseline correction. The cytotoxicity of the hydrogels and any leachable materials was also evaluated by using methyl thiazolyl tetrazolium (MTT) assay. Briefly, L929 cells were seeded at a density of 10⁴ per well in a 96-well plate and incubated for 24 h. The medium was replaced by the eluent of hydrogels or PEI 25K solution with a concentration at 0.125 mg/mL, which was used as a positive control. The cells were subjected to MTT assay after being incubated for another 24 h. The absorbance value at 490 nm was measured on a microplate reader. Cell viability (%) was calculated according to the followed equation: $\text{viability (\%)} = (A_{\text{sample}}/A_{\text{control}}) \times 100\%$, where A_{sample} and A_{control} are the absorbance of the sample and control well (without the eluent of hydrogels), respectively. The measurements were performed in triplicate.

In vivo degradation and biocompatibility

Sprague-Dawley (SD) rats (~200 g) were used for *in vivo* tests. Rats were anesthetized by inhalation of diethyl ether. PLG-g-TA/PEG solutions (10% (w/v), 500 μL for each sample) in PBS containing H₂O₂ (1.6 mM) and HRP (2 units/mL) were subcutaneously injected in the back of the rats. At predetermined time intervals, the rats were euthanized, and the gel status was observed. The tissues surrounding the injection sites were surgically removed and stored in neutral buffered formalin solution (NBF). The histology analysis was examined by staining with hematoxylin and eosin (H&E).

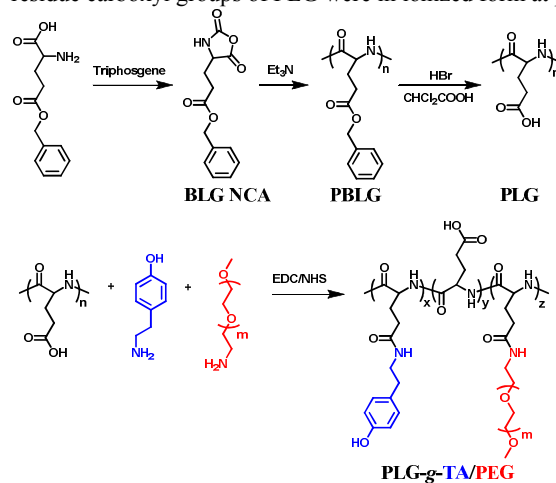
Animal procedure

The animal experiments were carried out according to the guide for the care and use of laboratory animals, provided by Jilin University, Changchun, China, and the procedure was approved by the local Animal Ethics Committee.

Results and discussion

Synthesis and characterization of PLG-g-TA/PEG copolymer

The synthetic route of PLG-g-TA/PEG copolymer is illustrated in Scheme 1. Poly(L-glutamic acid) (PLG) was synthesized by ring-opening polymerization (ROP) of BLG NCA with triethylamine as an initiator, followed by deprotection of the benzyl groups of PBLG using HBr solution (33 wt%) in acetic acid. Subsequently, TA and mPEG-NH₂ were grafted to the backbone of PLG *via* a carbodiimide active amidation reaction. The typical ¹H NMR spectra are shown in Figure 1. The disappearance of the peak of benzyl groups in PLG suggested the successful deprotection of PBLG (Figure 1A and 1B). The weight-average molecular weight (M_w) of PLG was evaluated to be 1.3×10^4 with a polydispersity index (PDI) of 1.28 by GPC. Based on the ¹H NMR spectrum of the graft copolymer (Figure 1C), in addition to the typical peaks assigned to PLG, the representative peaks ascribed to tyramine (TA) and PEG were also observed, indicating the successful synthesis of the PLG-g-TA/PEG copolymer. The grafting ratio of TA residues, defined as the number of TA moieties per 100 repeated units of L-glutamate, was calculated to be 20 by comparing the integration of the peak of TA (-C₆H₄-) at 6.8-7.0 ppm with that of methylene peak of glutamate unit (-CH₂CH₂C(O)-) at about 2.1 ppm (Figure 1C). Similarly, the grafting ratio of mPEG-NH₂ residues was calculated to be 28 based on the NMR results. The weight contents of TA and PEG were 3.9 wt% and 79.1 wt%, respectively. The conjugation of TA onto PLG was also examined by using UV-Vis spectrometer. The PLG-g-TA/PEG aqueous solution showed a specific absorbance peak at 277 nm, which corresponds to the absorbance of phenol moieties (Figure 2a). The content of conjugated TA was 4.5 wt%, which is consistent with the NMR results. Additionally, the conformation of PLG-g-TA/PEG in aqueous solution at pH 7.4 was examined by circular dichroism spectroscopy. As shown in Figure 2b, a small positive maximum at about 217 nm and a large minimum at about 204 nm were observed, indicating that PLG-g-TA/PEG adopted a random conformation.⁴⁶ The reason could be attributed to the fact that the residue carboxyl groups of PLG were in ionized form at pH 7.4.⁴⁶



Scheme 1 Synthetic route of PLG-g-TA/PEG copolymer.

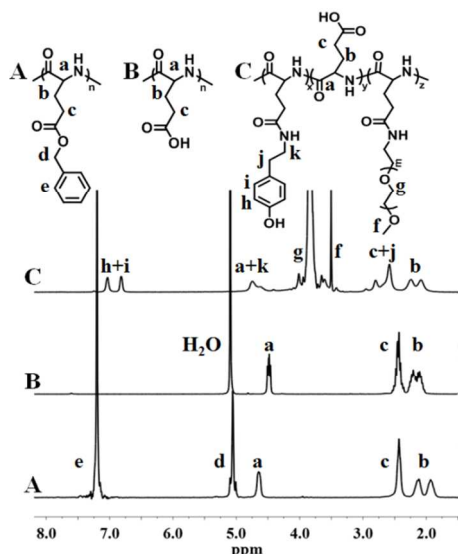


Fig.1 ^1H NMR spectra of (A) PBLG in CF_3COOD ; (B) PLG in D_2O ; (C) PLG-g-TA/PEG copolymer in CF_3COOD .

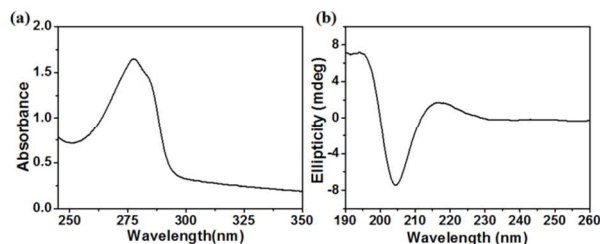
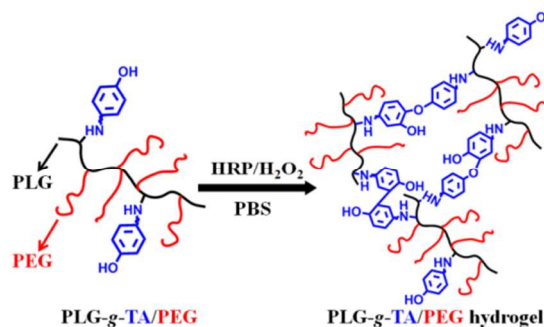


Fig.2 (a) UV-Vis absorbance spectrum of PLG-g-TA/PEG aqueous solution; (b) Circular dichroism spectrum of PLG-g-TA/PEG aqueous solution (pH 7.4).

Preparation and gelation time of the hydrogels

The hydrogels were prepared by HRP-mediated crosslinking of PLG-g-TA/PEG copolymer (Scheme 2). The coupling of phenol moieties in the PLG-g-TA/PEG copolymer *via* the carbon-carbon bonds or carbon-oxygen bonds was catalyzed by HRP and H_2O_2 , leading to the formation of intermolecular covalent linkages and the rapid formation of hydrogels. The gelation time was determined by the vial tilting method. The dependence of the gelation time on the concentrations of HRP and H_2O_2 is shown in Figure 3. The gelation time reduced from 135 to 23 s as the HRP concentration increased from 1.0 to 16.7 units/mL at fixed polymer concentration of 6.7% (w/v) and H_2O_2 concentration of 1.6 mM. This should be attributed to the fact that the increase in HRP concentration accelerated the generation of phenolic free radicals.^{25, 38} In contrast, as the H_2O_2 concentration increased from 0.8 to 8.2 mM, the gelation time prolonged from 80 to 150 s at a fixed HRP concentration of 4 units/mL. This phenomenon occurred due to the inhibition effect of excessive H_2O_2 on the activity of HRP.³⁸ The influence of HRP and H_2O_2 concentrations on the gelation time was consistent with some naturally derived systems, such as carboxymethylcellulose^{47, 48} and gelatin.^{28, 29} Notably, the hydrogels based on PLG-g-TA/PEG have been developed by using relatively low amounts of H_2O_2 , which may avoid toxic effects of H_2O_2 at high concentrations.⁴⁹ Additionally, it was found that the gelation time of PLG-g-TA/PEG hydrogels was tunable by changing the concentrations of HRP and H_2O_2 . The

control of gelation time is quite important for practical applications of the hydrogels.



Scheme 2 Schematic route of enzyme-mediated crosslinking of PLG-g-TA/PEG copolymer.

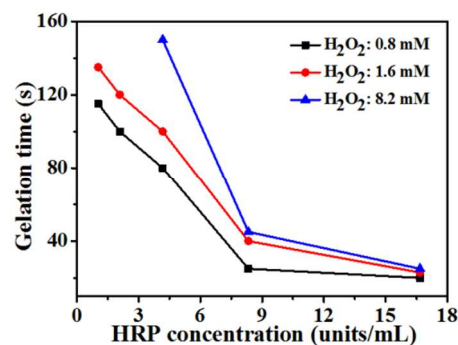


Fig.3 Dependence of gelation time of PLG-g-TA/PEG hydrogels on HRP and H_2O_2 concentrations.

Rheological experiments

The viscoelastic property of PLG-g-TA/PEG hydrogels was measured in a time-controlled oscillatory mode at 37 °C. A mixture of PLG-g-TA/PEG, HRP and H_2O_2 solutions in PBS was placed on the plate of rheometer. The formation of hydrogels was detected by monitoring the variations of storage modulus (G') and loss modulus (G'') with time. As shown in Figure 4a, the G' and G'' of PLG-g-TA/PEG hydrogels crosslinked with 2 units/mL of HRP and 1.6 mM of H_2O_2 were measured as a function of time. An immediate gelation was observed as soon as the mixture was placed on the plate of rheometer. Subsequently, the storage modulus of the hydrogels gradually increased during the initial stage and eventually reached a plateau, suggesting that the crosslinking reaction was complete.²⁰ As shown in Figure 4b, the storage modulus of PLG-g-TA/PEG hydrogels strengthened from 1600 to 2300 Pa with increasing the concentration of HRP from 1 to 4 units/mL at a fixed H_2O_2 concentration of 1.6 mM. This result indicated that HRP displayed a marked effect on the mechanical properties of the hydrogels.⁴⁰ Notably, the increase in H_2O_2 concentration led to higher storage modulus. This should be due to the fact that H_2O_2 acted as a crosslinker in this system and therefore the increase in H_2O_2 concentration led to the increase in the crosslinking density.³⁸ The results of rheological tests demonstrated that the mechanical properties of the hydrogels could be controlled by varying the HRP and H_2O_2 concentrations.

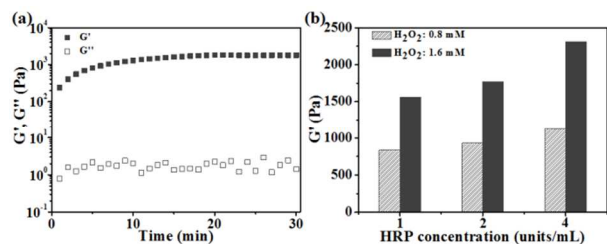


Fig.4 (a) Storage modulus (G') and loss modulus (G'') of PLG-g-TA/PEG hydrogels as a function of time with the presence of 2 units/mL of HRP and 1.6 mM of H_2O_2 ; (b) the effects of HRP and H_2O_2 concentrations on G' of PLG-g-TA/PEG hydrogels.

Morphology of lyophilized hydrogels

The morphology of lyophilized hydrogels was observed by SEM. As shown in Figure 5, the PLG-g-TA/PEG hydrogels exhibited interconnected porous structures. It was found that the pore size of the hydrogels was markedly influenced by the H_2O_2 concentration. For instance, the average pore-size of the hydrogel crosslinked with 0.8 mM of H_2O_2 and 2 units/mL of HRP ranged from 70 to 120 μm (Figure 5a). In contrast, the inner porous structure of the hydrogel crosslinked with 1.6 mM of H_2O_2 and 2 units/mL of HRP was more compact and the average pore-size ranged from 20 to 60 μm (Figure 5b). The decrease in the pore size as the increase in H_2O_2 concentration was due to a higher cross-linking density.³⁸ It is noteworthy that many studies have demonstrated that porous micro-structure with suitable pore size of hydrogel matrix played a critical role in cell survival, migration, proliferation and differentiation.⁵⁰ Furthermore, the pore size of hydrogels affected the release behavior of encapsulated drugs or bioactive molecules.²¹ In our study, the pore size of the PLG-g-TA/PEG hydrogels could be easily adjusted by the H_2O_2 concentration, which contributed to the further applications of the PLG-g-TA/PEG hydrogels.

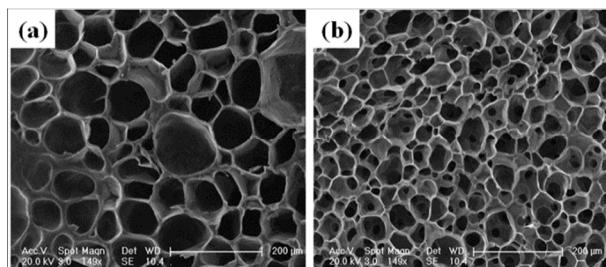


Fig.5 SEM images of lyophilized PLG-g-TA/PEG hydrogels crosslinked with (a) 0.8 mM of H_2O_2 and 2 units/mL of HRP, or (b) 1.6 mM of H_2O_2 and 2 units/mL of HRP. The scale bar represents 200 μm .

Swelling ratio of the hydrogels

The swelling behaviors of PLG-g-TA/PEG hydrogels formed with various HRP and H_2O_2 concentrations were determined by incubating the freeze-dried hydrogels in PBS at 37 $^{\circ}\text{C}$. The hydrogels were weighted at predetermined time intervals to obtain the swelling ratios. As shown in Figure 6, the hydrogels had high equilibrium swelling ratio ranging from 33 to 49, suggesting that freeze-dried PLG-g-TA/PEG hydrogels absorbed plenty of water because of the hydrophilic PEG segments. It was found that the equilibrium swelling ratio reduced as the H_2O_2 concentration increased from 0.8 to 1.6 mM (Figure 6a, Figure S2 in Supporting Information). Additionally, with the increase of HRP concentration

from 2 to 8 units/mL, the equilibrium swelling ratio decreased from 49 to 40 (Figure 6b). Generally, the swelling ratio is related to the crosslinking density of the hydrogels. An increase in the crosslinking density usually results in a decrease in the swelling ratio.⁵¹ The results suggested that, in our experimental range, the increases in the H_2O_2 and HRP concentrations led to the increase in the crosslinking density, which is coincident with the SEM observation (Figure 5).

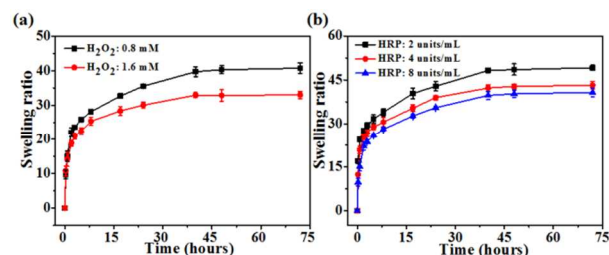


Fig.6 Swelling ratios of PLG-g-TA/PEG hydrogels: (a) HRP concentration fixed at 8 units/mL; (b) H_2O_2 concentration fixed at 0.8 mM ($n=3$).

In vitro cytocompatibility

L929 mouse fibroblasts were incubated inside the PLG-g-TA/PEG hydrogels formed with different concentrations of H_2O_2 and 2 units/mL of HRP. The cell viability was then determined by a live-dead cell staining kit. Cells were stained with calcein-AM/PI and observed by fluorescent microscope. As shown in Figure 7a, most of cells inside the hydrogels were stained green, indicating a high viability of the cells. The cell proliferation in the PLG-g-TA/PEG hydrogels was analyzed by cell counting kit-8 (CCK-8) method. The L929 cells in the hydrogel with lower H_2O_2 concentration exhibited a higher proliferation rate (Figure 7b), which may due to a higher porosity. The cytotoxicity of the hydrogels and any leachable materials was also evaluated by using MTT assay. The cell viability was over 90% after incubation with the eluent of the hydrogels, suggesting good cytocompatibility of the hydrogels (Figure 7c). It is worth mentioning that the low dose of H_2O_2 used in the PLG-g-TA/PEG hydrogels and the mild enzyme-mediated gelation process should contribute to the excellent cytocompatibility of the hydrogels.^{52,53}

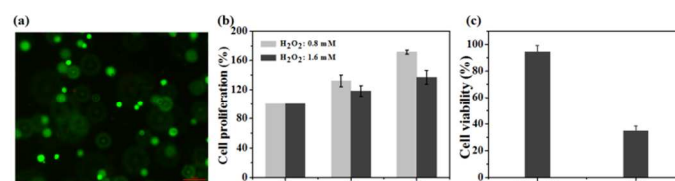


Fig.7 *In vitro* 3D culture of L929 cells. (a) Viability of L929 cells in the PLG-g-TA/PEG hydrogel with the presence of 1.6 mM of H_2O_2 and 2 units/mL of HRP after 1 day of incubation. Cells were stained with calcein-AM and PI. Live and dead cells show green and red fluorescence, respectively. The scale bar represents 100 μm . (b) Proliferation of L929 cells in the PLG-g-TA/PEG hydrogels analyzed by CCK-8 method. (c) Cell viability after exposure to the eluent of the PLG-g-TA/PEG hydrogels with PEI 25K as a positive control, normalized to that obtained on TCPS. ($n=3$).

In vivo degradation and biocompatibility

In order to investigate the *in vivo* degradation and biocompatibility of the PLG-g-TA/PEG hydrogels, 500 μL of PLG-g-TA/PEG solution in PBS containing H_2O_2 (1.6 mM) and HRP (2 units/mL)

was injected into the subcutaneous layer of rats. It was found that the hydrogels were rapidly formed *in situ* after subcutaneous injection of the PLG-g-TA/PEG solutions (Figure 8). The hydrogels persisted for up to 10 weeks *in vivo*, and completely degraded 14 weeks post-injection. The PLG-g-TA/PEG hydrogels in subcutaneous layer of the rats were mainly degraded due to the effects of mammalian proteolytic enzymes.^{54, 55}

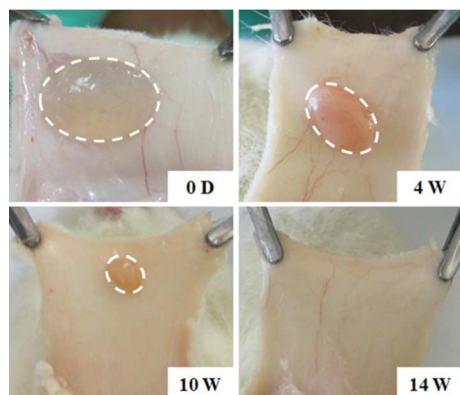


Fig.8 *In vivo* hydrogels status at different periods. PLG-g-TA/PEG solutions in PBS (10% (w/v)) containing H₂O₂ (1.6 mM) and HRP (2 units/mL) were subcutaneously injected into rats. Photos were taken at 15 min (0 day), 4, 10, 14 weeks.

Additionally, to investigate the biocompatibility of the hydrogels *in vivo*, the inflammatory response to the injected hydrogels was studied by hematoxylin and eosin (H&E) staining of the surrounding tissues at different time intervals. Elevated number of inflammatory cells were observed at first four weeks after injection (Figure 9), indicating mild inflammatory reaction in the initial stage.^{56, 57} Notably, inflammatory cells markedly reduced and the inflammatory reaction eliminated gradually along with the degradation of the hydrogels. Moreover, during our experiment, neither obvious tissue necrosis, edema, hyperemia and hemorrhaging, nor muscle damage were observed. Therefore, the results suggested that the PLG-g-TA/PEG hydrogels exhibited acceptable biocompatibility *in vivo*, indicating that the hydrogels have potential in some biomedical applications, such as tissue engineering scaffolds and carriers for long-term sustained delivery of drugs and bioactive molecules.

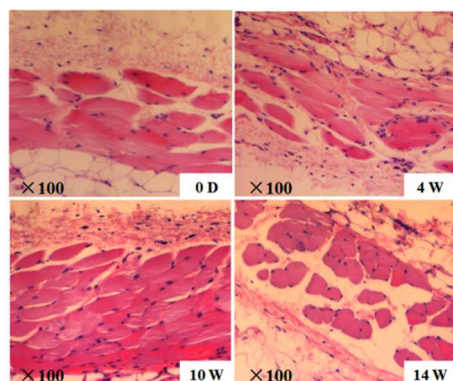


Fig.9 Histological images of tissues around the injection sites at the back of rats (H&E staining).

Conclusions

A kind of enzyme-mediated injectable hydrogels based on poly(L-glutamic acid) grafted with tyramine and poly(ethylene glycol) (PLG-g-TA/PEG) were developed. The hydrogels were rapidly formed under physiological conditions with the presence of HRP and H₂O₂. The gelation time could be adjusted by varying the concentrations of HRP and H₂O₂. The physicochemical properties of the hydrogels, including mechanical strength, swelling ratio and porous structure, were dependent on the concentrations of HRP and H₂O₂. The live-dead staining and cell counting kit-8 revealed that the PLG-g-TA/PEG hydrogels exhibited good cytocompatibility *in vitro*. The *in situ* formed hydrogels in the subcutaneous layer of rats persisted for up to 10 weeks and displayed acceptable biocompatibility *in vivo*. Therefore, the PLG-g-TA/PEG hydrogels could be promising candidates for biomedical applications, such as tissue engineering scaffolds and carriers for long-term sustained delivery of bioactive molecules.

Acknowledgments

The authors are grateful for the financial support from the National Natural Science Foundation of China (projects 51003103, 21174142, 51073154, 51233004 and 51321062), and the Ministry of Science and Technology of China (International cooperation and communication program 2011DFR51090).

Notes and references

^a Key Laboratory of Polymer Ecomaterials, Changchun Institute of Applied Chemistry, Chinese Academy of Sciences, Changchun 130022, P. R. China.

^b University of Chinese Academy of Sciences, Beijing 100039, P. R. China.

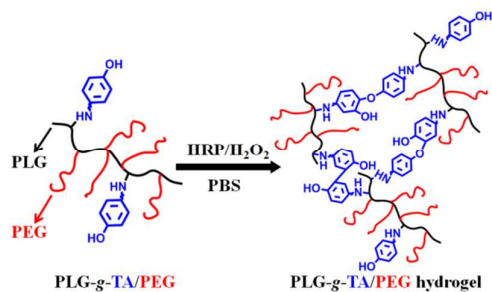
*Corresponding author, E-mail: clhe@ciac.ac.cn (C. He), ligao@ciac.ac.cn (G. Li)

1. D. Y. Ko, U. P. Shinde, B. Yeon and B. Jeong, *Progress in Polymer Science*, 2014, **38**, 672-701.
2. N. Annabi, A. Tamayol, J. A. Uquillas, M. Akbari, L. E. Bertassoni, C. Cha, G. Camci-Unal, M. R. Dokmeci, N. A. Peppas and A. Khademhosseini, *Advanced Materials*, 2014, **26**, 85-124.
3. J. Thiele, Y. Ma, S. M. C. Bruekers, S. Ma and W. T. S. Huck, *Advanced Materials*, 2014, **26**, 125-148.
4. C. He, S. W. Kim and D. S. Lee, *J Control Release*, 2008, **127**, 189-207.
5. L. Yu and J. Ding, *Chemical Society Reviews*, 2008, **37**, 1473-1481.
6. J. N. Hunt, K. E. Feldman, N. A. Lynd, J. Deek, L. M. Campos, J. M. Spruell, B. M. Hernandez, E. J. Kramer and C. J. Hawker, *Advanced Materials*, 2011, **23**, 2327-2331.
7. M. Lemmers, J. Sprakel, I. K. Voets, J. van der Gucht and M. A. Cohen Stuart, *Angewandte Chemie*, 2010, **122**, 720-723.
8. G. Song, L. Zhang, C. He, D.-C. Fang, P. G. Whitten and H. Wang, *Macromolecules*, 2013, **46**, 7423-7435.
9. Z. Zhang, J. Ni, L. Chen, L. Yu, J. Xu and J. Ding, *Biomaterials*, 2011, **32**, 4725-4736.
10. A. Gutowska, B. Jeong and M. Jasionowski, *The Anatomical Record*, 2001, **263**, 342-349.
11. H. Cui, J. Shao, Y. Wang, P. Zhang, X. Chen and Y. Wei, *Biomacromolecules*, 2013, **14**, 1904-1912.

12. K. T. Nguyen and J. L. West, *Biomaterials*, 2002, **23**, 4307-4314.
13. H. Park, X. Guo, J. S. Temenoff, Y. Tabata, A. I. Caplan, F. K. Kasper and A. G. Mikos, *Biomacromolecules*, 2009, **10**, 541-546.
14. A. S. Sawhney, C. P. Pathak and J. A. Hubbell, *Macromolecules*, 1993, **26**, 581-587.
15. C. Hiemstra, L. J. van der Aa, Z. Zhong, P. J. Dijkstra and J. Feijen, *Macromolecules*, 2007, **40**, 1165-1173.
16. C. Hiemstra, L. J. van der Aa, Z. Zhong, P. J. Dijkstra and J. Feijen, *Biomacromolecules*, 2007, **8**, 1548-1556.
17. G. N. Grover, J. Lam, T. H. Nguyen, T. Segura and H. D. Maynard, *Biomacromolecules*, 2012, **13**, 3013-3017.
18. L. S. M. Teixeira, J. Feijen, C. A. van Blitterswijk, P. J. Dijkstra and M. Karperien, *Biomaterials*, 2012, **33**, 1281-1290.
19. M. Kurisawa, J. E. Chung, Y. Y. Yang, S. J. Gao and H. Uyama, *Chem Commun*, 2005, **34**, 4312-4314.
20. F. Lee, J. E. Chung and M. Kurisawa, *Soft Matter*, 2008, **4**, 880-887.
21. F. Lee, J. E. Chung and M. Kurisawa, *J Control Release*, 2009, **134**, 186-193.
22. S. Sakai and K. Kawakami, *Acta Biomater*, 2007, **3**, 495-501.
23. S. Sakai and K. Kawakami, *J Biomed Mater Res A*, 2008, **85A**, 345-351.
24. R. Jin, C. Hiemstra, Z. Y. Zhong and J. Feijen, *Biomaterials*, 2007, **28**, 2791-2800.
25. R. Jin, L. S. M. Teixeira, P. J. Dijkstra, C. A. van Blitterswijk, M. Karperien and J. Feijen, *Biomaterials*, 2010, **31**, 3103-3113.
26. R. Jin, L. S. M. Teixeira, P. J. Dijkstra, C. A. van Blitterswijk, M. Karperien and J. Feijen, *J Control Release*, 2011, **152**, 186-195.
27. R. Jin, L. S. M. Teixeira, P. J. Dijkstra, Z. Y. Zhong, C. A. van Blitterswijk, M. Karperien and J. Feijen, *Tissue Eng Pt A*, 2010, **16**, 2429-2440.
28. K. M. Park, K. S. Ko, Y. K. Joung, H. Shin and K. D. Park, *J Mater Chem*, 2011, **21**, 13180-13187.
29. S. Sakai, K. Hirose, K. Taguchi, Y. Ogushi and K. Kawakami, *Biomaterials*, 2009, **30**, 3371-3377.
30. L. S. Wang, J. E. Chung, P. P. Y. Chan and M. Kurisawa, *Biomaterials*, 2010, **31**, 1148-1157.
31. L. S. Wang, C. Du, J. E. Chung and M. Kurisawa, *Acta Biomater*, 2012, **8**, 1826-1837.
32. R. Jin, L. S. M. Teixeira, P. J. Dijkstra, M. Karperien, C. A. van Blitterswijk, Z. Y. Zhong and J. Feijen, *Biomaterials*, 2009, **30**, 2544-2551.
33. E. Lih, J. S. Lee, K. M. Park and K. D. Park, *Acta Biomater*, 2012, **8**, 3261-3269.
34. S. Sakai, Y. Yamada, T. Zenke and K. Kawakami, *J Mater Chem*, 2009, **19**, 230-235.
35. N. Q. Tran, Y. K. Joung, E. Lih and K. D. Park, *Biomacromolecules*, 2011, **12**, 2872-2880.
36. N. Q. Tran, Y. K. Joung, E. Lih, K. M. Park and K. D. Park, *Biomacromolecules*, 2010, **11**, 617-625.
37. I. Jun, K. M. Park, D. Y. Lee, K. D. Park and H. Shin, *Macromol Res*, 2011, **19**, 911-920.
38. K. M. Park, Y. M. Shin, Y. K. Joung, H. Shin and K. D. Park, *Biomacromolecules*, 2010, **11**, 706-712.
39. Y. K. Joung, S. S. You, K. M. Park, D. H. Go and K. D. Park, *Colloids and Surfaces B: Biointerfaces*, 2012, **99**, 102-107.
40. K. M. Park, Y. Lee, J. Y. Son, D. H. Oh, J. S. Lee and K. D. Park, *Biomacromolecules*, 2012, **13**, 604-611.
41. T. J. Deming, *Progress in Polymer Science*, 2007, **32**, 858-875.
42. C. He, X. Zhuang, Z. Tang, H. Tian and X. Chen, *Advanced Healthcare Materials*, 2012, **1**, 48-78.
43. Y. Cheng, C. He, C. Xiao, J. Ding, X. Zhuang, Y. Huang and X. Chen, *Biomacromolecules*, 2012, **13**, 2053-2059.
44. C. Deng, J. Wu, R. Cheng, F. Meng, H.-A. Klok and Z. Zhong, *Progress in Polymer Science*, 2014, **39**, 330-364.
45. C. He, C. Zhao, X. Chen, Z. Guo, X. Zhuang and X. Jing, *Macromolecular Rapid Communications*, 2008, **29**, 490-497.
46. . Myer, P. Y. *Macromolecules* 1969, **2**, 624-628.
47. Y. Ogushi, S. Sakai and K. Kawakami, *J Biosci Bioeng*, 2007, **104**, 30-33.
48. S. Sakai, Y. Ogushi and K. Kawakami, *Acta Biomater*, 2009, **5**, 554-559.
49. B. Halliwell, M. V. Clement and L. H. Long, *FEBS Letters*, 2000, **486**, 10-13.
50. A. Leal-Egaña, A. Díaz-Cuenca and A. R. Boccaccini, *Advanced Materials*, 2013, **25**, 4049-4057.
51. X. Gao, Y. Cao, X. Song, Z. Zhang, X. Zhuang, C. He and X. Chen, *Macromol Biosci*, 2013, DOI: 10.1002/mabi.201300384.
52. R. Jin, C. Lin and A. Cao, *Polymer Chemistry*, 2014, **5**, 391-398.
53. R. Jin, B. Lou and C. Lin, *Polymer International*, 2013, **62**, 353-361.
54. C. Li, *Advanced Drug Delivery Reviews*, 2002, **54**, 695-713.
55. L. S. Nair and C. T. Laurencin, *Progress in Polymer Science*, 2007, **32**, 762-798.
56. Y. Cheng, C. He, C. Xiao, J. Ding, H. Cui, X. Zhuang and X. Chen, *Biomacromolecules*, 2013, **14**, 468-475.
57. E. Y. Kang, H. J. Moon, M. K. Joo and B. Jeong, *Biomacromolecules*, 2012, **13**, 1750-1757.

Injectable Enzymatically-crosslinked Hydrogels Based on Poly(L-glutamic acid) Graft Copolymer

Kaixuan Ren,^{a,b} Chaoliang He,^{a,*} Yilong Cheng,^a Gao Li,^{a,*} and Xuesi Chen^a



Enzyme-mediated injectable hydrogels based on a poly(L-glutamic acid) graft copolymer with tunable physicochemical properties, biodegradability and good biocompatibility were developed.